REVIEW ARTICLE

CrossMark

Dukono, the predominant source of volcanic degassing in Indonesia, sustained by a depleted Indian-MORB

Philipson Bani[1] · Giancarlo Tamburello[2] · Estelle F. Rose-Koga[1] · Marco Liuzzo[3] · Alessandro Aiuppa[4] · Nicolas Cluzel[1] · Iwan Amat[5] · Devy Kamil Syahbana[5] · Hendra Gunawan[5] · Marcello Bitetto[4]

Abstract
Located on Halmahera island, Dukono is among the least known volcanoes in Indonesia. A compilation of the rare available reports indicates that this remote and hardly accessible volcano has been regularly in eruption since 1933, and has undergone nearly continuous eruptive manifestation over the last decade. The first study of its gas emissions, presented in this work, highlights a huge magmatic volatile contribution into the atmosphere, with an estimated annual output of about 290 kt of SO_2, 5000 kt of H_2O, 88 kt of CO_2, 5 kt of H_2S and 7 kt of H_2. Assuming these figures are representative of the long-term continuous eruptive activity, then Dukono is the current most prominent volcanic gas discharge point in Indonesia and ranks among the top-ten volcanic SO_2 sources on earth. Combining our findings with other recent volcanic SO_2 flux results, obtained during periodic campaigns at a number of volcanoes with DOAS and UV-Cameras, the SO_2 emission budget for Indonesia is estimated at 540 kt year^{-1}, representing 2–3% of the global volcanic SO_2 contribution into the atmosphere. This figure should be considered as minimum as gas emissions from numerous other active volcanoes in Indonesia are yet to be evaluated. This voluminous degassing output from Dukono is sustained by a depleted Indian-MORB (I-MORB) mantle source. This latter is currently undergoing lateral pressure from the steepening of the subducted slab, the downward force from the Philippine Sea plate and the westward motion of a continental fragments along the Sorong fault, leading to high fluid fluxes to the surface. Over the course of Dukono eruptive activity, the magma reservoir has changed from a less differentiated source that fed the past voluminous lava flows to a more evolved melt that sustained the current ongoing explosive activity.

Keywords Dukono volcano · Degassing budget · Depleted mantle source · Magma source evolution

---

✉ Philipson Bani
philipson.bani@ird.fr

[1] Université Clermont Auvergne, CNRS, IRD, OPGC, Laboratoire Magmas et Volcans, F-63000 Clermont-Ferrand, France

[2] Istituto Nazionale di Geofisica e Vulcanologia, Sezione di Bologna, Via Donato Creti, 12, 40100 Bologna, Italy

[3] Istituto Nazionale di Geofisica e Vulcanologia, Sez, Palermo, Via Ugo La Malfa, 153 90146 Palermo, Italy

[4] Dipartimento di Scienze della Terra e del Mare (DiSTeM), Università di Palermo via archirafi, 36 90123 Palermo, Italy

[5] Center for Volcanology and Geological Hazard Mitigation (CVGHM), Jl. Diponegoro No. 57, Bandung, Indonesia

Introduction

Dukono is a complex volcano with overlapping craters that culminate at 1230 m above sea level. It is a rather broad and low profile edifice, surrounded by multiple inactive cones. The current activity is hosted in the main central crater of ~ 700 m in diameter. Located on the northern part of Halmahera island (Fig. 1), Dukono is the most active volcano in the Maluku region, and perhaps the currently most vigorously active volcano in Indonesia. The historical volcanic activity record, briefly summarized in Table 1, suggests strong eruptive discharges have persisted since 1933. A large eruptive event in 1550 devastated the once known city of Tolo (Data Dasar 2011; Van Padang 1983). During our visits in July and September 2015, Dukono exhibited nearly continuous
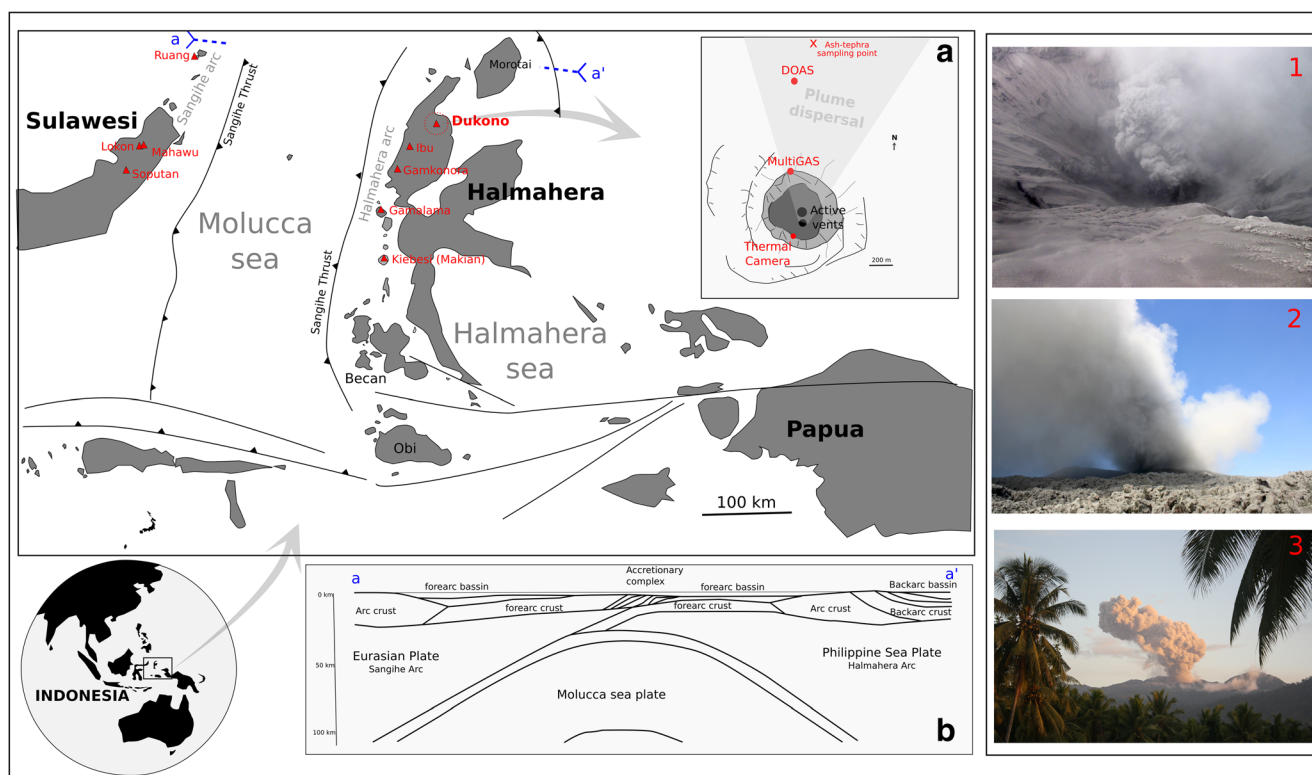
Fig. 1 Dukono volcano located on Halmahera island, east Indonesia. The crater hosts 2 active vents (**a**). The collision of the Halmahera and Sangihe arcs is highlighted in cross section a-a', adapted from Hall and Wilson (2000) (**b**). The measurement positions of the scanning DOAS and MutiGAS as well as the ash-tephra sampling points are indicated in (**a**). Pictures on the right provide an insight into Dukono crater (1), the ashy plume above the crater (2) and a strong eruptive discharge observed 10 km from the crater (3)

eruptive discharge from its two active vents, forming a persistent dense ashy plume up to 200–300 m above the crater, being dispersed to the north by the prevailing wind. The entire edifice was covered by thick ash deposits (up to a meter at some points) on its flanks.

Despite these remarkable accounts, Dukono is rarely visited, thus very little is known about its manifestations – the main constraints being the remoteness of the edifice and the difficulty of access. We present here the first gas study on Dukono with a focus on the emission budget and the origin of its magma source, using Multicomponent Gas Analyzer System (MultiGAS) and Differential Optical Absorption Spectroscopy (DOAS) measurements, combined with ash-tephra chemistry analysis.

Geological setting

The geodynamic of the Molucca sea is currently dominated by the collision of the Halmahera and Sangihe arcs (Fig. 1). The oceanic lithosphere that existed between the two arcs over last 20 million years has been entirely consumed (Cardwell et al. 1980). According to Hall and Wilson (2000), the Sangihe forearc is presently overriding the Halmahera forearc, while the Halmahera arc itself is thickening by the over-thrusting of

its back-arc from the east. The Molucca sea plate that once largely exposed to the surface between Sangihe and Halmahera arcs is now deep in the mantle and sinking further with time (Hall and Wilson 2000). The currently active volcanoes are formed along the weak points of the entire forearc-arc-backarc section of Halmahera region (Hall and Wilson 2000).

Methodology

MultiGAS

The Multi-GAS used in this work is a compact portable instrument from UniPa-INGV (as used by Aiuppa et al. 2015). The system simultaneously acquired concentrations of H_2O, CO_2, SO_2, H_2S and H_2 at 0.1 Hz. H_2O and CO_2 were detected by non-dispersive infrared spectroscopy (LI-COR LI-840A; 0–60,000 ppm range), and SO_2, H_2S and H_2 via specific electrochemical sensors (respectively, models 3ST/F, EZ3H, and EZT3HYT "Easy Cal"; all from City Technology with calibration range of 0–200 ppm). Powered by a (6 Ah) 12 V LiPo battery, this lightweight Multi-GAS was placed on the northern part of Dukono's crater (Fig. 1), directly in the plume. Nearly 3 h of continuous recording was achieved. Acquired

Table 1 Brief chronology of Dukono volcanic activity

1550	Large eruption spilling out huge amount of lava to the coast, destroying the once known Tolo city (Van Padang 1983).
1719	Eruptive activity on the eastern flank (GVP 2013)
1861–1869	Eruption at the main crater. Vegetation close to summit was destroyed by fire triggered by the eruption (Data Dasar 2011).
1901	Eruption occurred at the main crater whilst strong fumarole activity observed on the surrounding cones (Data Dasar 2011).
Aug. 1933	Strong eruption with large lava flow to the north and ash fall up to 15 km northeast of the volcano (Data Dasar 2011).
1945	Eruption leading to ash fall on Tobelo city, situated 15 km northeast of the volcano
Jul. 1946	Eruption generating ash fall on Morotai island, 60 km northeast of Dukono. At Tobelo, 1 cm of ash fall was observed (Data Dasar 2011).
1952	Eruption propelling an ash column up to ~ 1000 m from the summit. Eruption sound was heard in Tobelo (15 km from volcano) (Data Dasar 2011).
1969	Eruption building ash column. The explosion was heard at Galela (10 km from summit) (Data Dasar 2011).
1971	Eruption building up a black column of ash up to 300 m from summit. Ash fall at the summit (Data Dasar 2011).
1978–1979	Explosions of varying strength occurred about once every 10 s, ejecting bombs as large as 4 m up to 200–250 m from the crater rim. Ash emission was nearly continuous, with clouds rising as high as 10 km above the crater. Ash was blown North beyond the Galela, 15 km from the volcano. From Galela incandescent ejecta were visible (GVP 1978. Report on Dukono (Indonesia)).
Jun. 1991	Eruption generation ash column up to 1500 m above crater rim. Ash fall witnessed on Tobelo, lava glow seen at the summit at night whilst lahar occurred following the eruption (Data Dasar 2011).
May 1992	Eruption building up ash plume to 400 m above volcano (Data Dasar 2011).
Nov.-Dec. 1993	Eruption building up ash plume up to 300–600 m above summit (Data Dasar 2011). The cloud was rising up to 600–1500 m (GVP 1993. Report on Dukono (Indonesia)).
Jan., Sep. 1995	Eruption generating ash fall but weather condition did not allow detail observation (Data Dasar 2011).
Mar. – Dec. 2003	Eruption building up ash plume to 200–500 m above summit. Ash fall witnessed at Tobelo (Data Dasar 2011).
2004–2005	Continuous ash emission (GVP 2006. Report on Dukono (Indonesia).
2006–present	Intermittent ash emission with variable discharge intensity. In 2007 and 2014 the ash plume was clearly observed by MODIS (GVP 2007. Report on Dukono (Indonesia)

data were post-processed using the Ratiocalc program (Tamburello 2015).

DOAS measurements

DOAS measurements were performed from a fixed position about 800 m north of the active crater (Fig. 1) using a scanning system. The plume drifted to the north during DOAS measurements enabling a vertical scanning across the plume. 67 spectra were collected per scan with a step angle of 1.8°. The spectrometer used was an Ocean Optics USB2000+ with a spectral range of 290–440 nm and a spectral resolution of 0.5 FWHM. The SO_2 column amounts (ppm.m) were retrieved using DOAS calibration and standard analysis procedures (Platt and Stutz 2008). Reference spectra included in the non-linear fit were obtained by convolving high resolution SO_2 (Bogumil et al. 2003) and O_3 (Voigt et al. 2001) cross sections with the instrument line shape. A Fraunhofer reference spectrum and Ring spectrum, calculated in DOASIS, were also included in the fit. The total column amount of the plume cross section was then multiplied by the wind mean velocity of 5 m s^{-1}, obtained from hand-held anemometer on the crater rim, and assumed representative of the plume dispersion speed, to derive the SO_2 emission rate.

Ash-tephra sampling and laboratory analysis

At about 300 m north of the DOAS measurement point, 1 m of layered ash-tephra deposits are exposed to the surface (Fig. 1). Each layer was sampled then analyzed for bulk composition using X-ray Fluorescence (XRF) (Johnson et al. 1999) for major elements and compared to fresh ash fall (July and September 2015) samples. To gain further insights into the magmatic processes and source origin, major and trace elements of olivine, pyroxene and plagioclase hosted melt inclusions were analyzed using Electron Probe Micro Analyzer (EMP) (Cameca SX 100) following standard procedure (e.g. Le Voyer et al. 2008; Cabral et al. 2014). Analytical uncertainties on the samples were typically of < 2% for SiO_2, MgO, and Al_2O_3; 3.5% for FeO and CaO; 5% for K_2O, TiO_2, and Na_2O; 10% for P_2O_5; and 30% for MnO (1σ). F, S, and Cl were also measured by EMP with relative uncertainty of 20% for S and 30% for Cl and F. Trace element measurements were carried out using a laser ablation system (193 nm Excimer Resonetics M-50E) associated with an inductively coupled plasma mass spectrometer (Agilent 7500 cs; LA-ICPMS) (e.g. Rose-Koga et al. 2012). The relative 1σ standard errors are < 3% for Rb, Sr, Y, Zr, Nb, Ba, La, and Ce, < 4% for Nd, < 9% for Th.

Fig. 2 Scatter plots of SO_2 vs H_2 (**a**), CO_2 (**b**), H_2O (**c**) and H_2S (**d**); the correlation between H_2O and CO_2 is displayed (**e**). The SO_2 fluctuation over the recording period (**f**) with the corresponding FFT result (**g**) indicating a degassing periodicity of ~ 3 min
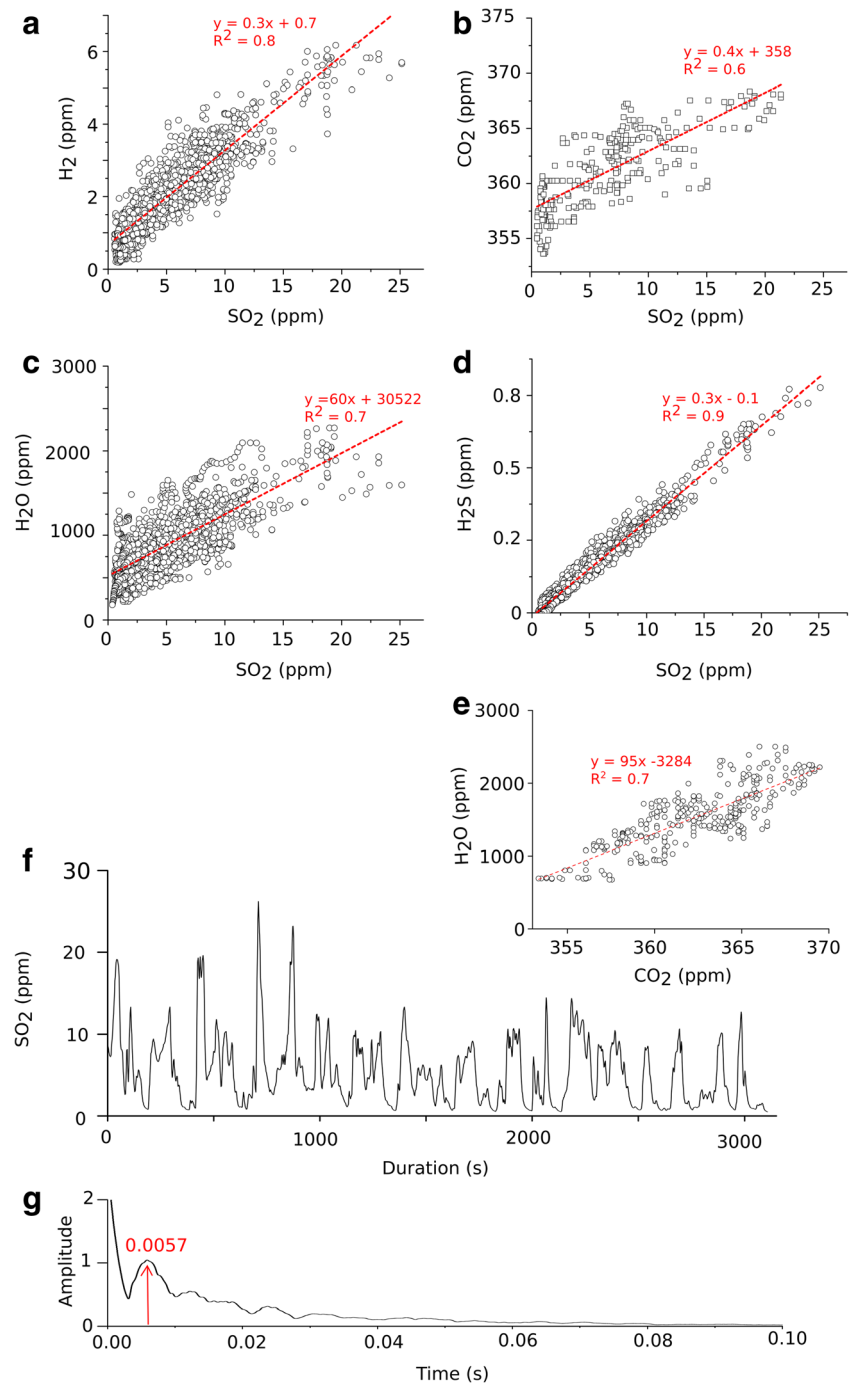
Results

Gas composition and emission rate

The position of the Multi-GAS, on the northern part of Dukono's crater rim (Fig. 1), enhanced direct exposure to eruptive gas discharges but also to heavy ash releases that subsequently saturated the filter after about 1 h of recording. Results, presented in Fig. 2 and Table 2, indicate strong fluctuations in SO_2 concentrations, varying from 0.5 to 32 ppm, with the alternation of 1–3 min of strong releases followed by 0.5–1 min of low background volcanic gas emission. FFT analysis indicates a degassing periodicity of $\sim$ 3 min. The data-set highlights a H_2O-rich gas composition from Dukono, representing a molar proportion of 97%. Other gases detected on Dukono are CO_2, H_2S and H_2 with mean recorded values of 362–400 ppmv, 0.2 ppmv (above atmospheric background) and 1–2 ppmv respectively

Table 2 Dukono gas composition, mean concentrations, gas ratios and fluxes

	13/07/2015	08/09/2015	Average
Gas concentration			
Mean SO_2 (ppm v)	5.3 ± 1.3	2.0 ± 0.5	3.6 ± 0.9
Mean H_2S (ppm v)	0.2 ± 0.05	0.2 ± 0.04	0.2 ± 0.04
Mean CO_2 (ppm v)	362 ± 90	400 ± 100	381 ± 95
Mean H_2 (ppm v)	2 ± 0.5	1.0 ± 0.2	1.5 ± 0.7
Mean H_2O (ppm v)	9000 ± 2200	8000 ± 2000	8500 ± 2100
H_2O/SO_2	60.5 ± 19.1	61.2 ± 22.1	60.8 ± 20.6
CO_2/SO_2	0.4 ± 0.1	0.6 ± 0.2	0.5 ± 0.1
H_2S/SO_2	0.03 ± 0.01	0.05 ± 0.02	0.03 ± 0.01
H_2/SO_2	0.3 ± 0.1	0.1 ± 0.07	0.2 ± 0.09
Gas composition and flux estimates			
	Composition (mol %)	Flux (t d^{-1})	
H_2O (mol. %)	97.2 ± 2.7	$14,000 \pm 4000$	
SO_2 (mol. %)	1.6 ± 0.4	819 ± 235	
CO_2 (mol. %)	0.8 ± 0.2	242 ± 69	
H_2S (mol. %)	0.06 ± 0.01	13 ± 4	
H_2 (mol. %)	0.30 ± 0.07	7 ± 2	

(Table 2). There is no gas composition change between our two observation periods (in July and September, 2015). All

these gases exhibit positive correlations with SO_2, implying a common source (Fig. 2).

SO_2 emission from Dukono was also very well characterized on the spectra acquired by DOAS scanning. The SO_2 emission rate, obtained after more than 2 h of vertical scanning, fluctuates between 400 and 2000 t d^{-1} with a mean SO_2 flux of 819 ± 235 t day^{-1} (Table 3; Fig. 3). The duration of one scan varied between 3 and 6 min, depending on the light intensity. The temporal resolution of the DOAS scans is therefore not high enough to resolve the possible degassing periodicity observed with the Multi-GAS. However the difference between the minimum and the maximum emission rates suggests that there are different phases of stronger and lower emissions.

Taking into account the molar ratios of H_2S/SO_2, H_2/SO_2, CO_2/SO_2, H_2O/SO_2 (Table 2) we obtain a daily output of 242 ± 69 t of CO_2, 13 ± 4 t of H_2S, 7 ± 2 t of H_2 and about $14,000 \pm 4000$ t of H_2O.

Ash-tephra and melt inclusion composition

Laboratory analyses result of the ash-tephra samples and melt inclusions are provided in Table 4. Figure 4 displays the composition changes in terms of alkali versus silica, allowing insights into the source composition. The bulk composition of ash-tephra deposits appear in the junction
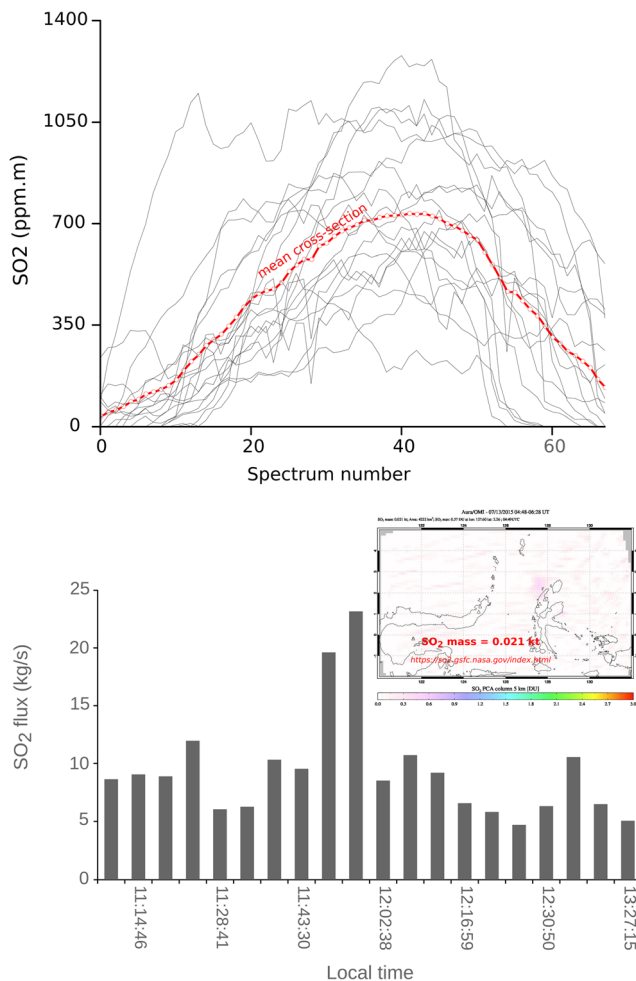
Table 3 SO_2 flux results obtained from scanning DOAS

Start time (LT) (date: Jul. 12, 2015)	End time (LT)	Number of spectra	Scanning step (°)	Mean column amount (ppm m)	SO_2 flux (t/d)
11:11:41	11:14:46	76	1.8	474	756 ± 220
11:14:46	11:16:32	76	1.8	619	992 ± 229
11:17:52	11:22:48	76	1.8	359	778 ± 223
11:24:03	11:28:31	76	1.8	325	1044 ± 289
11:28:41	11:32:57	76	1.8	534	530 ± 162
11:33:10	11:37:58	76	1.8	496	549 ± 170
11:38:08	11:43:20	76	1.8	1059	902 ± 255
11:43:30	11:48:44	76	1.8	1270	834 ± 243
11:51:59	11:57:14	76	1.8	452	1707 ± 470
11:57:27	12:02:28	78	1.8	642	2015 ± 541
12:02:38	12:06:24	76	1.8	589	745 ± 211
12:06:34	12:11:06	76	1.8	613	937 ± 265
12:11:17	12:16:48	76	1.8	332	804 ± 237
12:16:59	12:21:14	76	1.8	347	576 ± 163
12:21:25	12:26:13	76	1.8	392	510 ± 155
12:26:22	12:30:40	76	1.8	564	413 ± 124
12:30:50	12:35:26	76	1.8	362	553 ± 164
12:35:37	12:41:08	76	1.8	446	922 ± 274
12:48:12	12:53:22	76	1.8	446	569 ± 177
13:27:15	13:32:07	76	1.8	465	444 ± 137
Mean SO_2 flux = 819 ± 235					

Fig. 3 SO$_2$ scanning profiles across the plume; the mean profile is in red (above). Fluctuation of SO$_2$ flux over the DOAS scanning period (below). The sub-image displays the result obtained by OMI (Ozone Monitoring Instrument) for the same date as the DOAS measurement (July 13, 2015). This OMI image was acquired during DOAS measurements. The time difference between Universal Time Coordinated and Halmahera is 9 h

of trackyandesite and andesite whilst the melt inclusion compositions scattered from basalt to dacite with olivine-pyroxene-hosted melt inclusions plotted in the range of basalt and basaltic-andesite while the plagioclase-hosted melt inclusions spread along the transition line between andesite and trachyandesite and even up to differentiated dacitic composition. The volatile content (S, Cl, F) in the melt inclusions shows a notable drop of S from around 1100 ppm to 200–400 ppm between olivine-pyroxene and plagioclase hosts whilst Cl and F in contrast display relative increase from 600 to 800 to 1000–1200 ppm and from 200 to 300–700 ppm respectively (Fig. 5). Trace elements obtained from melt inclusions show elevated large ion lithophile elements (LILE) and light rare elements (LREE) compare to high-field strength elements (HFSEs). Nb and Ti are below N-MORB concentrations.

Discussion

Prominent volcanic gas contribution into the atmosphere

Due to the remote location and access difficulties, Dukono is one of the least known volcanoes in Indonesia and globally unknown to the scientific community—a paradox since this edifice is among the most active on earth (Table 1) with recurrent eruptive activity since 1933 (GVP 2013). In July then in September 2015 (this work), Dukono followed an eruptive manifestation (apparently normal according to local observers) with nearly continuous eruptive discharges from the two active vents in the crater. The mean SO$_2$ flux released from this activity amounts to 0.8 kt per day, which represents a mean annual SO$_2$ output into the atmosphere of 292 ± 86 kt. This figure is much lower than the daily 1.7 kt of SO$_2$ release from Dukono indicated in Carn et al. (2017), based on satellite observations. Although the two SO$_2$ flux approaches are not exactly equivalent, since we are measuring the emission rates directly whilst satellites output an SO$_2$ atmospheric burden, the two results should be at least comparable (Bani et al. 2009a, b) or lower for the Ozone Monitoring Instrument (OMI) onboard Aura satellite (McCormick et al. 2012; Bani et al. 2016). This satellite-based high SO$_2$ flux derived from a longer observation period (several years) but might be biased by over-sampling more vigorous (and most visible) explosive periods (Carn et al. 2016). The OMI estimation for July 13, 2015 is 0.02 kt which is an order of magnitude lower than our DOAS result for that same day (Fig. 3). Other DOAS measurements in the future are required to refine these first estimates, however our finding suggests that Dukono volcanic gas contribution into the atmosphere is higher than any other known persistent volcanic degassing source in Indonesia, measured with modern tools (DOAS and UV-Camera), including Merapi (18–160 kt year^{-1}; Surono et al. 2012), Krakatau (70 kt year^{-1}; Bani et al. 2015), Kawah Ijen (64 kt year^{-1}; Gunawan et al. 2016), Bromo (60 kt year^{-1}; Aiuppa et al. 2015), Semeru (20–70 kt year^{-1}; Smekens et al. 2015), Sirung (17 kt year^{-1}; Bani et al. (2017)) and Papandayan (0.5 kt year^{-1}; Bani et al. 2013). If put in the context of the well-known compilation of Andres and Kasgnoc (1998), the Dukono's SO$_2$ contribution into the atmosphere is comparable to that of Kilauea, in the top ten of the volcanic degassing sources worldwide. Combining together the above SO$_2$ emission data from 7 Indonesian volcanoes, one obtains a minimum annual volcanic SO$_2$ output of 540 kt into the atmosphere, representing 2–3% of the global volcanic emission budget (15–21 Tg; Halmer et al. 2002). This figure is much higher than the 100 kt of SO$_2$ emission budget provided by Andres and Kasgnoc (1998) or 120 kt in Fischer (2008) for the whole Indonesian volcanoes. Knowing that there are 127 active volcanoes in Indonesia, it is thus evident that these past figures are strongly underestimating the volcanic degassing

Table 4 Composition of Dukono bulk ash-tephra deposits and major to trace elements content of olivine-pyroxene-plagioclase-hosted melt inclusion

Bulk composition

	Fresh ash (Jul 2015)	Fresh ash (Sep 2015)_1	Fresh ash (Sep 2015)_2	Layer A	Layer B	Layer C	Layer D	Layer 1	Layer 2	Layer 3	Layer 4	Layer 5	Layer 6	Layer 7
SiO_2 (wt%)	58.0	59.5	59.3	59.0	58.9	58.9	58.9	59.4	59.2	58.4	59.6	59.0	59.4	58.7
TiO_2	0.8	0.8	0.7	0.7	0.7	0.7	0.7	0.7	0.7	0.8	0.7	0.7	0.7	0.7
Al_2O_3	13.9	15.3	15.8	14.5	14.2	14.1	14.2	14.3	14.3	13.5	14.4	14.2	14.5	15.0
Fe_2O_3	10.5	8.4	8.6	9.4	9.9	10.1	1.0	9.4	9.5	11.2	9.2	9.8	9.1	9.0
MnO	0.2	0.2	0.1	0.1	0.1	0.2	0.2	0.2	0.1	0.2	0.1	0.1	0.1	0.1
MgO	2.0	2.7	2.3	2.2	2.7	2.6	2.6	2.1	1.9	3.5	2.1	2.6	2.0	1.8
CaO	7.3	5.8	6.0	6.8	6.4	6.6	6.5	6.5	6.7	6.4	6.4	6.5	6.6	7.0
Na_2O	3.1	3.4	3.5	3.3	3.3	3.3	3.3	3.3	3.4	3.3	3.4	3.4	3.3	3.5
K_2O	3.7	2.5	2.5	3.3	3.1	3.2	3.2	3.4	3.5	3.0	3.3	3.2	3.4	3.3
P_2O_5	0.4	0.3	0.3	0.4	0.4	0.4	0.3	0.4	0.4	0.3	0.4	0.4	0.4	0.3
SO_3	0.2	–	–	0.0	0.0	0.0	0.0	0.1	0.1	0.1	0.1	0.1	0.0	0.0
Total	100.1	98.9	99.1	99.7	99.7	100.1	90.9	99.8	99.8	100.7	99.7	100	99.5	99.4

Melt inclusions

	ol-1	ol-1	cpx-1	cpx-2	plagio-1	plagio-2	plagio-3	plagio-4	plagio-5	plagio-6	plagio-7
SiO_2 (wt%)	52.9	52.5	50.8	55.1	59.7	60.0	60.3	61.0	61.9	63.0	64.2
TiO_2	0.7	0.6	0.7	0.6	1.0	0.8	0.9	0.9	0.8	0.9	0.8
Al_2O_3	18.5	18.0	17.2	16.5	14.6	15.1	14.8	14.8	14.5	14.9	14.9
FeO	6.3	6.6	9.1	5.8	8.0	7.4	7.9	7.4	7.3	7.0	6.1
MnO	0.0	0.2	0.3	0.2	0.2	0.1	0.2	0.2	0.1	0.1	0.1
MgO	3.1	4.4	4.5	4.1	2.2	2.3	2.1	2.3	2.0	1.4	1.4
CaO	9.7	9.4	8.9	7.8	4.9	4.8	4.5	4.7	4.3	4.1	3.7
Na_2O	3.2	3.1	2.7	2.8	3.5	3.5	3.8	3.7	3.7	3.8	3.9
K_2O	1.4	1.3	0.7	1.3	3.0	2.9	3.2	3.1	3.4	3.4	3.6
P_2O_5	0.3	0.2	0.2	0.2	0.7	0.4	0.5	0.7	0.4	0.5	0.4
Total	96.2	96.4	95.0	94.4	97.9	97.4	98.3	98.8	98.5	99.3	99.0
H_2O (wt%)	3.8	3.6	5.0	5.6	2.1	2.6	1.7	1.2	1.5	0.7	0.9
Cl (ppm)	741.0	720.0	576.0	780.0	981.0	1178.0	1065.0	960.0	974.0	1230.0	1050.0
F	200.0	190.0	178.0	173.0	336.0	540.0	626.0	536.0	699.0	359.0	226.0
S	1120.0	1090.0	1119.0	1100.0	298.0	240.0	307.0	395.0	228.0	289.0	287.0
Li (ppm)	<4.7	11.2	29.9	49.8	83.4	57.3	21.2	55.7	19.5	24.3	20.8
V	269.2	259.3	361.7	293.9	180.8	213.0	171.7	157.9	154.5	146.2	93.7
Cr	41.5	49.9	<8.7	12.5	<7.1	<9.1	<6.9	<6.5	<8.7	<9.2	<6.8

Table 4 (continued)

Bulk composition

|											
Co	21.3	21.0	29.8	19.5	22.6	19.5	16.3	18.1	18.5	15.1	11.9
Ni	14.8	14.1	12.2	10.6	5.8	7.1	3.7	4.8	4.3	5.3	5.6
Rb	25.2	24.4	9.7	12.3	67.3	40.5	49.6	55.7	52.7	62.8	58.5
Sr	476.3	469.3	354.1	466.6	293.3	282.7	255.7	283.1	254.1	273.8	234.2
Y	15.7	15.0	21.5	11.9	40.8	21.1	29.4	31.1	21.3	33.9	34.7
Zr	60.5	59.9	51.0	47.1	190.0	83.1	117.6	132.5	86.4	152.4	159.2
Nb	0.9	0.9	0.6	0.7	3.1	1.3	1.8	2.1	1.4	2.4	2.4
Ba	213.9	214.1	116.3	165.6	462.4	365.5	406.3	432.6	404.0	463.0	534.5
La	6.7	6.7	8.0	6.7	15.9	8.7	11.6	13.4	10.2	15.1	14.9
Ce	15.0	14.6	19.5	15.9	37.1	19.3	27.2	30.3	21.7	32.7	33.5
Nd	9.6	9.4	12.1	9.0	24.2	12.7	18.8	19.8	14.3	21.6	21.4
Sm	2.3	2.5	2.8	1.9	6.3	3.4	4.3	5.1	3.5	5.8	5.3
Eu	0.8	0.7	1.0	0.7	1.6	1.0	1.2	1.4	1.2	1.6	1.5
Gd	2.9	2.6	3.0	1.9	6.8	3.2	4.5	5.5	3.6	6.0	5.9
Yb	1.6	1.7	2.5	1.5	4.4	2.6	3.2	3.0	2.2	3.6	4.0
Lu	0.3	0.3	0.4	0.2	0.6	0.4	0.5	0.5	0.3	0.5	0.6
Pb	6.6	6.4	3.9	4.5	14.8	11.5	11.5	11.7	11.8	15.3	14.0
Th	1.0	1.0	0.5	0.5	3.1	1.4	2.1	2.3	1.4	2.6	2.6
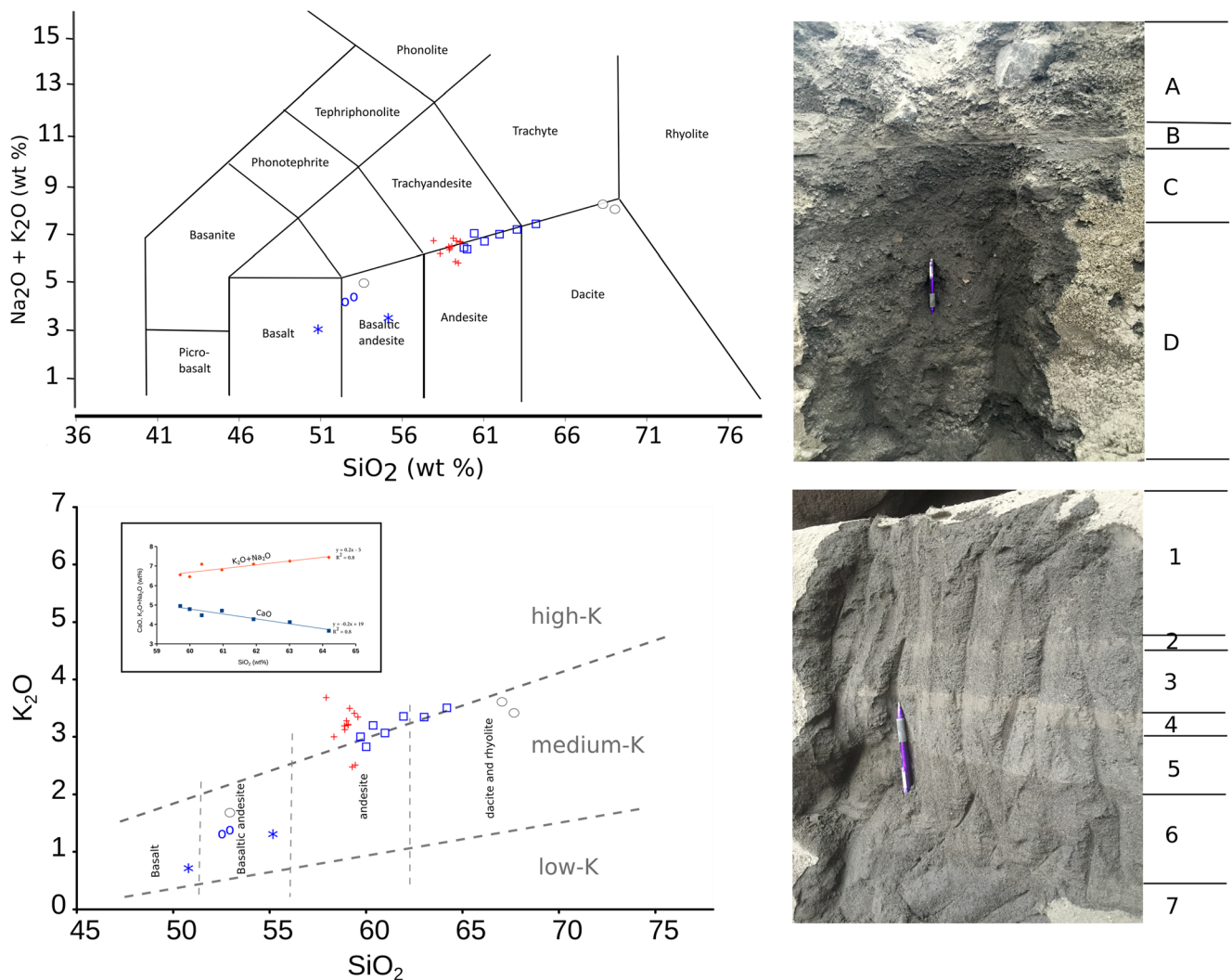
Fig. 4 Ash-tephra and melt inclusion samples placed into the total alkali and K_2O versus SiO_2 plots indicate andesite-trachyandesite with medium to high-K bulk composition (red cross), basaltic andesite olivine (blue circle), basalt to basaltic andesite pyroxene (blue asterisk) and andesite-trachyandeiste plagioclase (blue square). This latter shows an extend to higher SiO_2. White circles indicate Ibu volcano bulk composition changes for comparison. The subplot (on the K_2O-SiO_2 plot) denotes the evolution of plagioclase composition, from high Ca low Na (anorthite) to high Na low Ca (albite). The pictures on the right are the ash-tephra layer sampled and analyzed. The detail composition of the layers (A, B, C, 1, 2, 3, 4, 5) are provided in Table 3. The white circles denote the melt composition change observed on Ibu, the closest volcano to Dukono (Saing et al. 2014)

budget from this archipelago. Indeed, the most recent estimation provided by Carn et al. (2017) based on satellite observations, indicates a much higher release with an annually SO_2 emission budget of around 2200 kt, representing about 10% of the global volcanic SO_2 contribution into the atmosphere (23 Tg; Carn et al. 2017). However this figure still requires ground-based validation in Indonesia. Note also that only 16 out of 127 volcanoes are considered in this latter work. .

The daily H_2O flux from Dukono estimated in this work is fairly high and accounts for $\sim 14 \pm 4$ kt (~ 5000 kt year^{-1}). This figure derives directly from the H_2O-rich signature of volcanic gas vented from Dukono. Indeed, the H_2O molar proportion is 97% (Table 2), which falls in the upper domain for arc volcanic gases (Fischer 2008) and is comparable, to,

e.g., Bromo (H_2O mol. 95%; Aiuppa et al. 2015) or Yasur (H_2O mol. 98%; Metrich et al. 2011). Note that the H_2O flux likely constitutes higher bound estimate since a meteoric water contribution to the Dukono degassing system cannot be ruled out. However the fairly strong correlation between H_2O and the other gases, including CO_2, SO_2, H_2S and H_2 (Fig. 2), suggests a primarily magmatic H_2O source. The high water proportion (4–5 wt%) calculated by weight difference from melt inclusions and its positive correlation with S content (Table 4; Fig. 5) supports the magmatic origin of H_2O.

CO_2 is the second most common gas in volcanic exhalations (e.g., Shinohara 2008). This is also the case on the three better known Indonesian volcanoes, including Bromo, Papandayan and Merapi, where CO_2 represents 3.5 mol%

Fig. 5 Volatile contents in melt inclusions (**a**). The Cl concentration shows a progressive increase with the increasing SiO_2 (green triangle). F evolved from a relatively stable concentration in low SiO_2 melt (black cross) to higher content with a more differentiated melt. The S highlights a notable drop with the increasing SiO_2, similar to the calculated H_2O. Incompatible element abundance in the olivine-pyroxene-plagioclase-hosted melt inclusions, normalized to N-MORB (**b**)
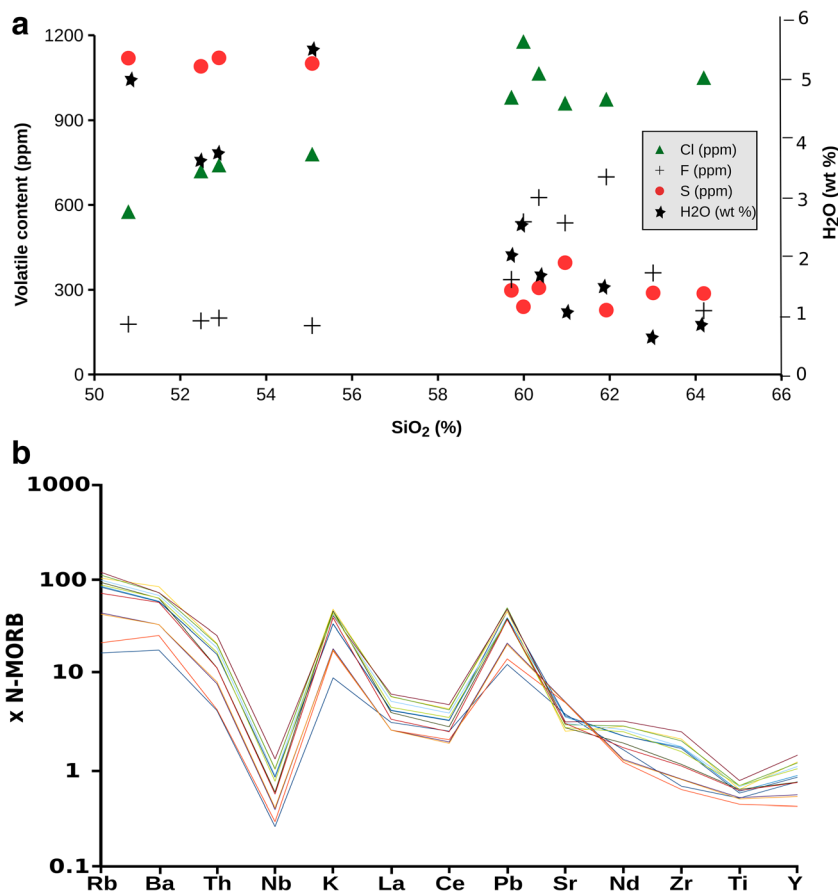
(Aiuppa et al. 2015), 2.9 mol% (Giggenbach 1996) and 4.7–5.6 mol% (Giggenbach et al. 2001) in their respective volcanic gas. But on Dukono, the CO_2 constitutes the 3rd most abundant gas composition with only 0.7 mol% behind H_2O and SO_2 (1.6 mol%). Using the CO_2/SO_2 ratio of (Table 2), we derive an annual CO_2 emission rate of 88 kt from Dukono. Such release represents ∼ 0.03% of the global volcanic CO_2 emission budget (271 Mt. $year^{-1}$; Burton et al. 2013) into the atmosphere. Further investigations are still required to constrain this low CO_2 signature at Dukono, however, using the CO_2/SO_2 and H_2S/SO_2 ratios of 0.5 and 0.03 respectively (Table 2), one can derive a CO_2/S_T ratio of 0.4, corresponding to group 2 volcanoes in the Aiuppa et al. (2017) classification, suggesting a de-volatilized slab source.

Another gas species quantified in the plume of Dukono is the H_2. It constitutes 0.4 M % of the emitted gas and a H_2/SO_2 molar ratio of 0.3. Combining this latter ratio with the SO_2 flux, we estimate an annual H_2 emission budget of 2.5 ± 0.7 kt (Table 2). To date, still very few measurements have captured the molecular hydrogen in the plume, thus much is yet required to provide acceptable estimation of global volcanic H_2 output into the atmosphere. In any case, Dukono is a significant source of molecular hydrogen into the atmosphere.

The H_2S, also measured in Dukono plume, has a fairly strong correlation with other gas species (Fig. 2). It constitutes 0.05 M % of Dukono gas composition. The mean H_2S/SO_2 ratio is 0.03, which gives an annual output estimation of 13 ± 4 kt, representing 0.03–0.8% of the global volcanic H_2S output (1500–37,100 kt; Halmer et al. 2002) into the atmosphere.

The quantification of Indonesian volcanic volatile contributions into the atmosphere still remains sparse as the emissions from other volcanoes are yet to be measured. However, Dukono is clearly a strong volcanic volatile contributor into the atmosphere, at the global scale. Taken into account its long eruptive manifestation, as highlighted by Carn et al. (2016), it is plausible that Dukono may constitute the biggest volcanic degassing source in Indonesia.

A depleted I-MORB source and high fluid fluxing

The trace elements in melt inclusions (this work) normalized to normal mid-ocean ridge basalt (N-MORB) (Sun and McDonough 1989) point out elevated ratios of large ion lithophile elements (LILEs) and light rare elements (LREEs) to the high-field strength elements (HFSEs) (Fig. 6a). Such patterns observed at Dukono are typical of subduction zones in which the mantle wedge has been contaminated by fluids released from the subduction slab (McCulloch and Gamble 1991; Davidson 1996; Macpherson et al. 2003).

Fig. 6 (**a**) Zr/Nb vs MgO of Dukono (this work, red asterisk) compared to Obi, Central Halmahera and Becan (data from Macpherson et al. 2003). (**b**) Ba/Nb vs Zr/Nb of Dukono (this work, red asterisk) compared to central Halmahera and I-MORB (data from Macpherson et al. 2003). Note that Macpherson et al. (2003) observed an evolution in melt composition on Halmahera between Neogene and Quaternary. (**c**) The Halmahera $^{208}Pb/^{204}Pb$ and $^{206}Pb/^{204}Pb$ rocks plotted on Indian MORB. Note the increase in the $^{208}Pb/^{204}Pb$ and $^{206}Pb/^{204}Pb$ ratios between Neogene and Quaternary (data from Macpherson et al. 2003)
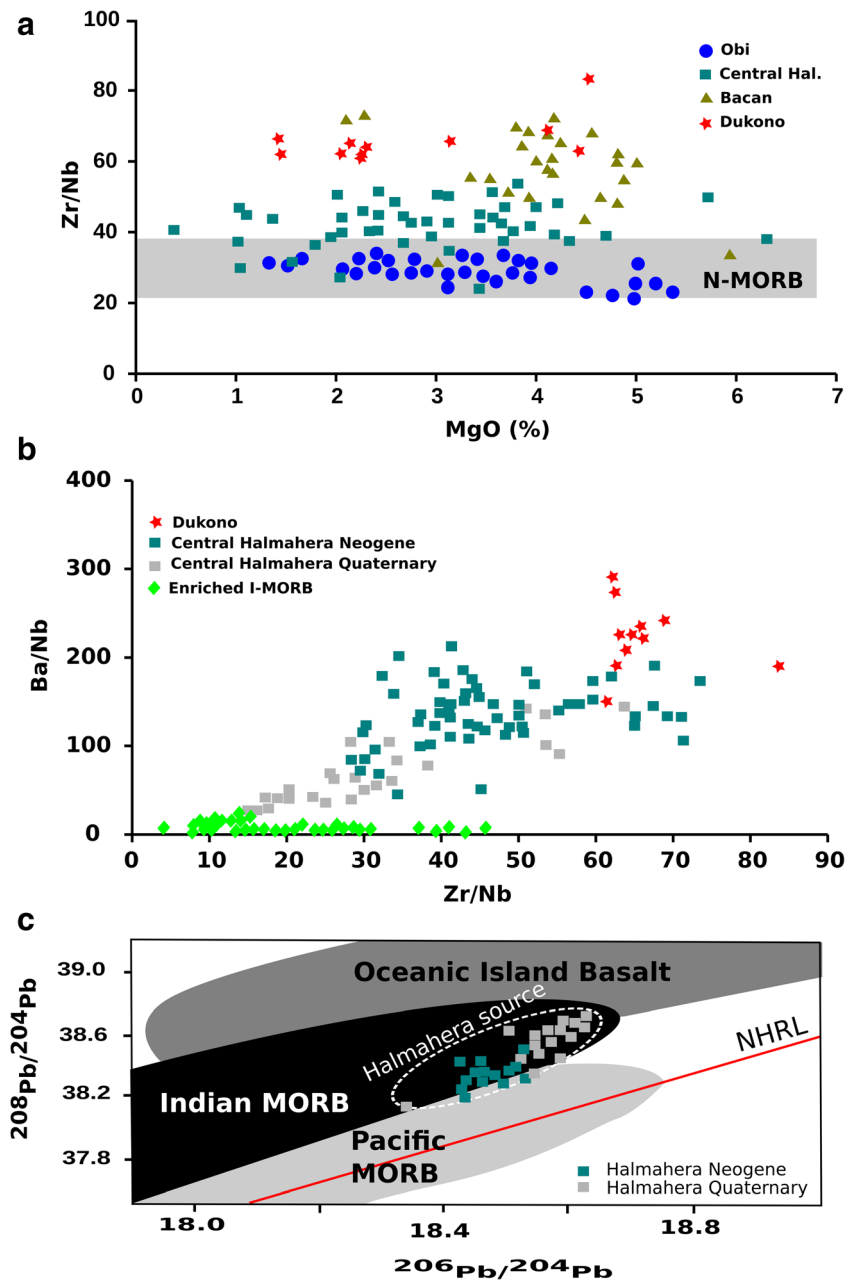
It is known that during slab de-volatilization, Nb and Zr are relatively immobile. The MORB sources display a restricted range of Zr/Nb (Fig. 6a) (e.g., Elliott et al. 1997), whilst at subduction zones, Zr/Nb can vary significantly (e.g., McCulloch and Gamble 1991), as seen at Halmahera (Fig. 6b). A high Zr/Nb cannot be generated by MORB-source (Woodhead et al. 1993). Instead, it characterizes mantle that has previously lost a basaltic melt fraction, leaving behind a source that is more depleted in highly incompatible elements, such as Nb (Macpherson et al. 2003). It is thus likely that this high Zr/Nb on Dukono derived from a depleted mantle wedge (Fig. 6b) in agreement with the changes in Zr/Nb ratios along the Halmahera arc, from N-MORB range (low Zr/Nb) at Obi

to an evolved mantle wedge source at Bacan and central Halmahera (Fig. 1; Fig. 6a; Macpherson et al. 2003).

A refractory source requires high fluid fluxes to lower the solidus and assist the melting process, therefore a high Zr/Nb ratio suggests important fluid fluxing. Further, given the high mobility of Ba, any incoming fluid into a depleted mantle source will produce a broad correlation between Zr/Nb and Ba/Nb (Fig. 6b) (e.g., Keppler 1996; Macpherson et al. 2003). The high ratios and strong correlation between Zr/Nb and Ba/Nb obtained at Dukono (Fig. 6b) thus support the idea of high fluid fluxes that sustain volcanic activity. The steepening of the subducted slab, the downward force from the Philippine sea plate and the westward motion of a continental fragments along

the Sorong fault (Fig. 1), are the main tectonic motions that can enhance mantle wedge compression beneath Halmahera (Macpherson et al. 2003; Elliott et al. 1997) leading to high fluid fluxes. These motions were evidenced in the evolution of Zr/Nb and Ba/Nb ratios at Halmahera between Neogene and Quaternary (Macpherson et al. 2003). Indeed the ratios decline and shift toward the enriched I-MORB composition (Fig. 6b) (Dosso et al. 1988; Le Roex et al. 1989) suggesting a progressive change from a depleted to enriched mantle source. Further, the steepening of the slab increases the effects of slab rollback in the mantle, leading to an increasing flux of recycled sediment as highlighted by the increase of $^{208}Pb/^{204}Pb$ at a given point of $^{206}Pb/^{204}Pb$ (Fig. 6d, Macpherson et al. 2003). Note here that the scatter plot of $^{207}Pb/^{204}Pb$ and $^{206}Pb/^{204}Pb$ ratios for Halmahera volcanic rocks indicate Indian-MORB source (e.g., Macpherson et al. 2003).

Evolved magma source

During fractional crystallization, melt inclusions, trapped in series of minerals, behave as closed and isolated systems, retaining much of the original composition of the melt, including their volatile content. Therefore, they constitute an ideal tool to shed light on the source of the magma and on igneous processes (e.g., Schiano 2003; Cannatelli et al. 2016). In that respect, the melt inclusion results obtained in this work (Fig. 4, Table 4) clearly trace back the fractional crystallization of Dukono magmatic source. The bulk chemistry of the ash-tephra deposits (Table 4), plotted in the total alkali-versus-silica (TAS) and K2O-silica diagrams (Fig. 4), indicate andesitic to tranchyandesitic magma composition with medium to relatively high-K content. Olivine-pyroxene-plagioclase-hosted melt inclusions show a wider range of compositions from basalts to tranchyandesites (Fig. 4, Table 4), an indication of a melt composition change in the reservoir. The plagioclase content shows a clear evolution with increasing SiO_2, from Ca-rich to Na-rich composition (Fig. 4). Such change generally reflect the continuous branch of Bowens's reaction series where calcium-rich plagioclase crystallizes first then progressively evolves to sodium-rich with the cooling melt (e.g., Monroe and Wicander 2014). The melt inclusion volatiles show a progressive increase of Cl and F, from 600 to 1000 ppm and from 200 ppm to > 200–700 ppm respectively (Fig. 5), implying incompatible behavior during crystal fractionation (Aiuppa et al. 2009). Fluorine has a high affinity for silicate melts, thus it may progressively enriched in magma through time as magmatic differentiation takes place (Sawyer and Oppenheimer 2006). Sulfur concentrations in Dukono inclusions show a notable drop from 1100 to ~ 300 ppm suggesting sulfur lost, likely through open-system degassing. All those observations indicate that the magmatic source beneath Dukono has evolved over time and that the current ongoing explosive activity is sustained by a more differentiated magma, which contrast with the voluminous lava outputs reported in the past (1550 and 1933; Table 1) likely sourced by a less viscous and less differentiated melt source.

Conclusions

Dukono is the most active volcano in Maluku and likely the most vigorous edifice in Indonesia with continuous and long eruptive manifestations. But due to its isolation and access difficulties, very little is known about its activity. The first measurements of its magmatic volatile contribution into the atmosphere, presented in this work, indicate that Dukono is the biggest volcanic SO_2 contributor in Indonesia and ranks among the top ten volcanic SO_2 sources on earth. Each year about 290 kt of SO_2 are released into the atmosphere from this volcano, a huge contribution that significantly increases the Indonesia archipelago annual volcanic SO_2 budget from 100 kt (Andres and Kasgnoc 1998) to 540 kt (including all recent published measurement results). This new Indonesian SO_2 emission budget constitutes 2–3% of the global volcanic SO_2 emission. The CO_2 released from Dukono appears to be much lower than the SO_2 output with 88 kt year^{-1}, representing 0.03% of global volcanic CO_2 budget. Dukono also releases annually about 5000 kt of H_2O, 41 kt of H_2S, and 0.4 kt of H_2 into the atmosphere.

The current degassing regime on Dukono is maintained by the ongoing explosive activity, enhanced by a differentiated magmatic source. Indeed, as evidenced in this work, the melt source has changed over the course of Dukono eruptive activity, evolving from a less viscous source that fed the past voluminous lava flows to a silica-rich melt behind the current ongoing explosive activity. In parallel to this differentiated melt source, trace element analyses highlight a depleted Indian-MORB in the mantle wedge beneath Dukono, a paradox behind the high degassing of Dukono. However, as highlighted in this work, the steepening of the subducted slab, the downward force from the Philippine sea plate and the westward motion of a continental fragments along the Sorong fault may develop sufficient pressure on the mantle wedge to enable high fluid fluxes to the surface.

References

Aiuppa A, Baker DR, Webster JD (2009) Halogens in volcanic systems. Chem Geol 263(1-4):1–18. https://doi10.1007/10.1016/j.chemgeo.2008.10.005

Aiuppa A, Bani P, Moussallam Y, Di Napoli R, Allard P, Gunawan H, Hendrasto M, Tamburello G (2015) First determination of magma-derived gas emissions from Bromo volcano, eastern Java (Indonesia). J Volcanol Geotherm Res 304:206–213. https://doi10.1007/10.1016/j.jvolgeores.2015.09.008

Aiuppa A, Fischer TP, Plank T, Robidoux P, Di Napoli R (2017) Along-arc, inter-arc and arc-to-arc variations in volcanic gas SO_2/S_T ratios reveal dual source of carbon in arc volcanism. Earth Sci Rev 168: 24–47. https://doi10.1007/10.1016/j.earscirev.2017.03.005

Andres RJ, Kasgnoc AD (1998) A time-average inventory of subaerial volcanic sulfur emissions. J Geophys Res 103(D19):25251–25261. https://doi10.1007/10.1029/98JD02091

Bani P, Join J-L, Cronin SJ, Lardy M, Rouet I, Garaebiti E (2009a) Characteristics of the summit lakes of Ambae volcano and their potential for generating lahars. Nat Hazards Earth Syst Sci 9(4): 1471–1478. https://doi.1007/10.5194/nhess-9-1471-2009

Bani P, Oppenheimer C, Tsanev VI, Carn SA, Cronin SJ, Crimp R, Charley D, Lardy M, Robert TR (2009b) Surge in sulphur and halogen degassing from Ambrym volcano, Vanuatu. Bull Volcanol 71(10):1159–1168. https://doi10.1007/10.1007/s00445-009-0293-7

Bani P, Surono HM, Gunawan H, Primulyana S (2013) Sulfur dioxide emissions from Papandayan and Bromo, two Indonesian volcanoes. Nat Hazards Earth Syst Sci 13(10):2399–2407. https://doi.org/10.5194/nhess-13-2399-2013

Bani P, Normier A, Bacri C, Allard P, Gunawan H, Hendrasto M, Surono TV (2015) First evaluation of sulfur dioxide degassing from Anak Krakatau volcano, Indonesia. J Volcanol Geotherm Res 302:237–241. https://doi.org/10.1016/j.jvolgeores.2015.07.008

Bani P, Boudon G, Balcone-Boissard H, Delmelle P, Quiniou T, Lefèvre J, Garaebiti Bule E, Shinohara H, Lardy M (2016) The 2009-2010 eruption of Gaua volcano (Vanuatu archipelago): eruptive dynamics and unsuspected strong halogens source. J Volcanol Geotherm Res 322:63–75. https://doi.org/10.1016/j.jvolgeores.2015.06.023

Bani P, Alfianti H, Aiuppa A, Oppenheimer C, Sitinjak P, Tsanev V, Saing UB (2017) First study of heat and gas buget for Sirung volcano, Indonesia. Bull Volcanol 79(8):60. https://doi.org/10.1007/s00445-017-1142-8

Bogumil K, Orphal J, Homann T, Voigt S, Spietz P, Fleischmann OC, Vogel A, Harmann M, Kromminga H, Bovensmann H, Frerick J, Burrows JP (2003) Measurements of molecular absorption spectra with SCIAMACHY preflight model: instrument characterization and reference data for atmospheric remote sensing in the 230-2380 nm region. J Photochem Photobiol A 157(2-3):167–184. https://doi.org/10.1016/S1010-6030(03)00062-5

Burton MR, Sawyer GM, Granieri D (2013) Deep carbon emissions from volcanoes. Rev Mineral Geochem 75(1):323–354. https://doi.org/10.2138/rmg.2013.75.11

Cabral RA, Jackson MG, Koga KT, Rose-Koga EF, Hauri EH, Whitehouse MJ, Price AA, Day JMD, Shimizu N, Kelley KA (2014) Volatile cycling of H 2O, CO 2, F, and Cl in the HIMU mantle: a new window provided by melt inclusions from oceanic hot spot lavas at Mangaia, Cook Islands. Geochem Geophys Geosyst 15(11):4445–4467. https://doi.org/10.1002/2014GC005473

Cannatelli C, Doherty AL, Esposito R, Lima A, De Vivo B (2016) Understanding a volcano through a droplet: a melt inclusion approach. J Geochem Expl 171:4–19. https://doi.org/10.1016/j.gexplo.2015.10.003

Cardwell RK, Isacks BL, Karig DE (1980) The spatial distribution of earthquakes, focal mechanism solutions and subducted lithosphere in the Philippine and northeast Indonesian islands. Am Geophys Union Geophys Monogr 23:1–36

Carn SA, Clarisse L, Prata AJ (2016) Multi-decadal satellite measurements of global volcanic degassing. J Volcanol Geotherm Res 311: 99–134. https://doi.org/10.1016/j.jvolgeores.2016.01.002

Carn SA, Fioletov VE, McLinden CA, Li C, Krotkov NA (2017) Adecade of global volcanic SO_2 emissions measured from space. Sci Rep 7:44095. https://doi.org/10.1038/srep44095

Data Dasar Gunung api Indonesia (2011) Kementerian Energi dan Sumber daya Mineral, Badan Geologi. edisi kedua, 401–410

Davidson JP (1996) Deciphering mantle and crustal signatures in subduction zones. In: Bebout GE, Scholl DW, Kirby SH, Platt JP (eds) Subduction: top to bottom, vol 96. American Geophysical Union Monograph, pp 251–262

Dosso L, Bougault H, Beuzart P, Calcez JY, Joron JL (1988) The geochemical structure of the southeast Indian ridge. Earth Planet Sci Lett 88(1-2):47–59. https://doi.org/10.1016/0012-821X(88)90045-3

Elliott T, Plank T, Zindler A, White W, Bourdon B (1997) Element transport from slab to volcanic front at the Mariana arc. J Geophys Res 102(B7):14991–15019. https://doi.org/10.1029/97JB00788

Fischer TP (2008) Fluxes of volatiles (H2O, CO2, N2, Cl, F) from arc volcanoes. Geochem J 42(1):21–38. https://doi.org/10.2343/geochemj.42.21

Giggenbach WF (1996) Chemical composition of volcanic gases. In: Tilling R, Scarpa R (eds) IAVCEI-UNESCO: monitoring and mitigation of volcano hazards. Springer-Verlag, Berlin Heidelberg

Giggenbach WF, Tedesco D, Sulisiyo Y, Caprai A, Cioni R, Favara R, Fischer TP, Hirabayashi J, Korzhinsky M, Martini M, Menyailov I, Shinohara H (2001) Evaluation of results from forth and fifth IAVCEI field workshop on volcanic gases, Vulcano Island, Italy and Java, Indonesia. J Volcanol Geotherm Res 108:283–202

Global Volcanism Program (1978) Report on Dukono (Indonesia). In: Squires D (ed) Scientific event alert network bulletin, 3:8. Smithsonian Institution. http://dx.doi.org/10.5479/si.GVP.BGVN199306-268010

Global Volcanism Program (1993) Report on Dukono (Indonesia). In: Venzke E (ed) Bulletin of the global volcanism network, 18:6. Smithsonian Institution. http://dx.doi.org/10.5479/si.GVP.BGVN199306-268010

Global Volcanism Program (2006) Report on Dukono (Indonesia). In: Wunderman R (ed) Bulletin of the global volcanism network, 31: 6. Smithsonian Institution. https://dx.doi.org/10.5479/si.GVP.BGVN200606268010

Global Volcanism Program (2007) Report on Dukono (Indonesia). In: Wunderman R (ed), Bulletin of the global volcanism network, 32: 10. Smithsonian Institution. https://dx.doi.org/10.5479/si.GVP.BGVN200710268010

Global Volcanism Program (2013) Dukono (268010) in Volcanoes of the World, v. 4.6.3. In: Venzke E (ed) Smithsonian Institution. Downloaded 25 Nov 2017 (http://volcano.si.edu/volcano.cfm?vn=268010). https://doi.org/10.5479/si.GVP.VOTW4-2013

Gunawan H, Caudron C, Pallister J, Primulyana S, Christenson B, McCausland W, Van Hinsberg V, Lewicki J, Rouwet D, Kelly P, Kern C, Werner C, Johnson JB, Utami SB, Syahbana DK, Saing U, Suparjan PBH, Sealing C, Cruz MM, Maryanto S, Bani P, Laurin A, Schmid A, Bradley K, Agung Nandaka IGM, Hendrasto M (2016) New insights into Kawah Ijen's volcanic system from the wet volcano workshop experiment. Geol Soc Lond, Spec Publ 437(1):35–56. https://doi.org/10.1144/SP437.7

Hall R, Wilson MEJ (2000) Neogene sutures in eastern Indonesia. J Asian Earth Sci 18:781–808

Halmer MM, Schmincke HF, Graf HF (2002) The annual volcanic gas input into the atmosphere, in particular into the stratosphere: a global data set for the past 100 years. J Volcanol Geoth Res 115:511–528

Johnson DM, Hooper PR, Conrey RM (1999) XRF Analysus of rocks and minerals for major and trace elements on a single low dilution Li-tetraborate fused bead. JCPDS-International Centre for Diffraction Data

Keppler H (1996) Constraints from partitioning experiments on the composition of subduction zone fluids. Nature 380(6571):237–240. https://doi.org/10.1038/380237a0

Le Roex AP, Dick HJB, Fisher RL (1989) Petrology and geochemestry of MORB from 25°E to 46°E along the southwest Indian ridge: evidence for constrasting styles of mantle enrichment. J Petrol 30(4): 947–986. https://doi.org/10.1093/petrology/30.4.947

Le Voyer M, Rose-Koga EF, Laubier M, Schiano P (2008) Petrogenesis of arc lavas from the Rucu Pichincha and Pan de Azucar volcanoes (Ecuadorian arc): major, trace element, and boron isotope evidences from olivine-hosted melt inclusions. Geochem Geophys Geosyst 9(12). https://doi.org/10.1029/2008GC002173

Macpherson CG, Forde EJ, Hall R, Thirlwall MF (2003) Geochemical evolution of magmatism in an arc-arc collision: the Halmahera and Sangihe arcs, eastern Indonesia. In: Larter RD, Leat PT (eds) Intra-oceanic Subduction systems: tectonic and magmatic processes, vol 219. Geological Society, London, Special Publications, pp 207–220. https://doi.org/10.1144/GSL.SP.2003.219.01.10

McCormick BT, Edmonds M, Mather TA, Carn SA (2012) First synoptic analysis of volcanic degassing in Papua New Guinea. Geochem Geophys Geosyst 13(3):Q03008. https://doi.org/10.1029/2011GC003945

McCulloch MT, Gamble JA (1991) Geochemical and geodynamical constraints on subduction zone magmatims. Earth Planet Sci Lett 102(3-4):358–374. https://doi.org/10.1016/0012-821X(91)90029-H

Metrich N, Allard P, Aiuppa A, Bani P, Bertagnini A, Shinohara H, Parello F, Di Muro A, Garaebiti E, Belhadj O, Massare D (2011) Magma and volatile supply to post-collapse renewed volcanism and block resurgence in Siwi caldera (Tanna,Vanuatu arc). J Petrol 52(6): 1077–1105. https://doi.org/10.1093/petrology/egr019

Monroe JS, Wicander R (2014) The changing earth, exploring geology and evolution, 7th edn. Cengage Learning, Stamford

Platt U, Stutz J (2008) Differential optical absorption spectroscopy, Principles and Applications. Springer, 597 pp

Rose-Koga EF, Koga K, Schiano P, Le Voyer M (2012) Mantle source heterogeneity for south Tyrrhenian magmas revealed by Pb isotopes and halogen contents of olivine-hosted melt inclusions. Chem Geol 334:266–279. https://doi.org/10.1016/j.chemgeo.2012.10.033

Saing UB, Bani P, Kristianto (2014) Ibu volcano, a center of spectacular dacite dome growth and long-term continuous eruptive discharges. J Volcanol Geotherm Res 282:36–42. https://doi.org/10.1016/j.jvolgeores.2014.06.011

Sawyer GM, Oppenheimer C (2006) Chapter 5: volcanic fluorine emissions: observations by Fourier transform infrared spectroscopy. Adv Fluorine Sci 1:165–185. https://doi.org/10.1016/S1872-0358(06)01005-0

Schiano P (2003) Primitive mantle magmas recorded as silicate melt inclusions in igneous minerals. Earth Sci Rev 63(1–2):121–144. https://doi.org/10.1016/S0012-8252(03)00034-5

Shinohara H (2008) Excess degassing from volcanoes and its role on eruptive and intrusive activity. Rev Geophys 46(4):RG4005. https://doi.org/10.1029/2007RG000244

Smekens JF, Clarke AB, Burton MR, Harijoko A, Wibowo HE (2015) SO_2 emissions at Semeru volcano, Indonesia: characterization and quantification of persistent and periodic explosive activity. J Volcanol Geotherm Res 300:121–128. https://doi.org/10.1016/j.jvolgeores.2015.01.006

Sun S-S, McDonough WF (1989) Chemical and isotopic systematics of oceanic basalts. In: Saunders AD, Norry MJ (eds) Magmatism in the ocean basins, vol 42. Geological Society, London, Special Publications, pp 313–345. https://doi.org/10.1144/GSL.SP.1989.042.01.19

Surono et al (2012) The 2010 explosive eruption of Java's Merapi volcano—a '100-year' event. J Volcanol Geotherm Res 241–242(2012): 121–135. https://doi.org/10.1016/j.jvolgeores.2012.06.018

Tamburello G (2015) Ratiocalc: software for processing data from multicomponent volcanic gas analyzers. Comput Geosci 82:63–67. https://doi.org/10.1016/j.cageo.2015.05.004

Van Padang N (1983) History of volcanology in the east indies. Scr Geol 71:1–76

Voigt S, Orphal J, Bogumil K, Burrows JP (2001) The temperature dependence (203–293 K) of the absorption cross-sections of O_3 in the 230–850 nm region measured by Fourier-transform spectroscopy. J Photochem Photobiol A 143(1):1–9. https://doi.org/10.1016/S1010-6030(01)00480-4

Woodhead JD, Eggins S, Gamble JA (1993) High field strenght and transition element systematics in island arc and back-arc basin basalt: evidence for multi-phase melt extraction and a depleted mantle wedge. Earth Planet Sci Lett 114(4):491–504. https://doi.org/10.1016/0012-821X(93)90078-N